Crystallization in Polymer Melt Spinning

RAKESH K. GUPTA and KIM F. AUYEUNG, *Department of Chemical Engineering, State University of New York at Buffalo, Buffalo, New York 14260*

Synopsis

The crystallization behavior of poly(ethylene) terephthalate (PET) melt spun into fiber monofilaments was examined using a laboratory set-up. The wind-up speeds ranged from free fall under gravity to 1500 m/min. The major additional variables that were manipulated included the mass flow rate and the filament temperature profile. The structure of the as-spun fibers was probed using tensile tests, differential scanning calorimetry, optical birefringence, and x-ray diffraction. It was found that while the filaments that had been spun nonisothermally were essentially amorphous, those that had been made under isothermal conditions at temperatures ranging from 180°C to 240°C were oriented and crystalline. In addition, the rate of oriented crystallization was much greater than that under quiescent conditions at the same temperature. This is perhaps the first published study which shows that highly crystalline (up to 40% crystallinity) PET fibers can be obtained at low spinning speeds merely by altering the fiber temperature profile while the material is still above the polymer glass transition temperature.

INTRODUCTION

The phase transformation behavior, both free and induced, of crystallizable polymers has been studied in the past as a fundamental problem in materials science and also as a means of altering the mechanical properties of these substances. Although low molecular weight materials either crystallize or do not crystallize, long-chain molecules with an ordered chemical structure can usually crystallize, but whether they actually do so, and to what extent, depends on the physical conditions such as temperature, stress, and the nature of the environment. Furthermore, the size, orientation, and disposition of the crystals again depend on the processing conditions. Several reviews of the entire subject of polymer crystallinity are available,[1-3] and the specific topic of stress-induced crystallization has been discussed in a number of symposia,[4-7] to which the reader is referred for details of work on specific polymers or under specific conditions.

It is well established that in flowing polymer melts, chain alignment and extension occur, with an elongational flow field being more effective than a shear field for the purpose. For crystallizable polymers, the process of chain alignment and extension results in an increase in the rate of crystallization and also in a change in the crystal morphology from spherulitic to extended chain.[8,9] In the melt spinning of crystallizable polymers, these two structural processes proceed simultaneously. Chain alignment occurs in the direction of the fiber axis and the amount of chain extension is governed by the velocity gradient and the residence time. The former quantity can be increased by increasing the wind-up speed, but this decreases the residence time so that the effect of the increased velocity gradient is, to a large extent, negated. Nonethe-

Journal of Applied Polymer Science, Vol. 34, 2469–2484 (1987)
© 1987 John Wiley & Sons, Inc. CCC 0021-8995/87/072469-16$04.00

less, by this method alone, polyethylene terephthalate, (PET) a commercially important polymer, can be altered from a purely amorphous state to a highly crystalline state during high speed spinning.[10-12]

Molecular orientation and extension are affected by another important variable, namely the temperature, through its influence on the polymer relaxation time. Lowering temperature raises the relaxation time and retards thermal disorientation. As a consequence, a decrease in temperature must be equivalent to an increase in the velocity gradient as far as polymer chain extension is concerned and similar effects must be observed insofar as the crystallization behavior is concerned. In fact, controlling the temperature may be more effective since, in this case, the residence time remains essentially unchanged, and it was to study the influence of spin line temperature on the crystallization behavior that the present research was undertaken.

Polymer Used

The polymer used in this work was polyethylene terephthalate supplied by the Celanese Research Company (Summit, NJ). According to the manufacturer, it contained no dye, and it had an intrinsic viscosity of 0.65 dl/g. The number average molecular weight was 20,000 and the weight average molecular weight was 40,000 as determined by gel permeation chromatography (GPC). Due to the hygroscopic nature of PET, the polymer pellets were dried in a vacuum oven at 110°C for 16 hours and cooled under vacuum to room temperature before being used in the melt-spinning experiments.

The choice of this polymer was governed by several considerations. It is a commercially important polymer and is used to make synthetic fibers. It has a glass transition temperature (about 75°C) which is above room temperature, and this allows one to carry out the structure determination off-line without fear of additional structural changes. Finally, and most importantly, the use of this polymer yields amorphous fibers in typical industrial operations which run at wind-up speeds of about 3,000 m/min. The presence of crystals in fibers made at still lower speeds would therefore be a validation of the ideas proposed here.

Melt-Spining Set-Up and Procedure

The fiber spinning set-up consisted of an extruder, a metering pump, an isothermal chamber, and a winder. In addition, a camera, a cathetometer, and a modified pyrometer were used to observe the spinline and to measure the diameter and the temperature during the process of fiber formation. A schematic of the complete apparatus is shown in Figure 1.

The polymer was extruded through a killion screw extruder having a 1.9 cm diameter and 30 cm long screw. The extruder was equipped with a nitrogen-purged hopper through which dry polymer pellets were fed. The molten polymer was extruded into a metering pump from where it flowed through a capillary spinneret having a single orifice of 0.074 cm inner diameter and an L/D ratio of 3.

Under nonisothermal spinning conditions, the fiber was passed over a guide roll, wrapped around a feed roll, and finally wound up on a bobbin using a Leesona 967 winder. The total spinline length was about 2 meters. For

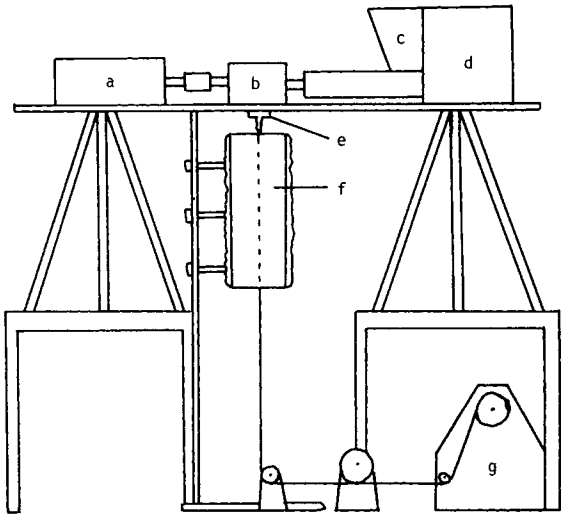

Fig. 1. Schematic diagram of the melt-spinning apparatus: (a) gear pump drive; (b) gear pump; (c) hopper purged with Nitrogen gas; (d) extruder; (e) spinneret; (f) insulated isothermal oven; and (g) winder.

isothermal spinning, a portion of the spinline between the spinneret and the guide roll was enclosed in a isothermal chamber of 7 cm diameter. The filament was cooled before entering the isothermal oven to a desired temperature (between 180°C and 240°C) and it was maintained at that temperature inside the chamber. As soon as it emerged from the chamber, it was rapidly cooled to room temperature using crossflow air generated by a fan. The finished fibers were collected and immediately stored in a glass vacuum desiccator for later analysis.

The isothermal chamber was constructed with two brass pipes telescoped together in such a way that the total length could be adjusted from 31 cm to 70 cm. On both sides of the chamber, running from top to bottom, a line of 18 holes, 1.27 cm in diameter and 3.18 cm apart were drilled and covered with two strips of pyrex glass having the same radius of curvature. These holes permitted observation of the spinline for the purpose of diameter determination. The oven itself was heated by band heaters that were strapped around the chamber.

The spinline temperature was measured with the help of a copper-constantan thermocouple using a null deflection technique. The running filament was contacted with a heated thermocouple and, depending on the temperature difference, heat would flow from or to the filament. This temperature difference could be sensed by a millivolt potentiometer connected to the thermocouple. By repeated applications of this procedure, a fairly accurate estimate of the fiber temperature could be achieved. More details can be found in the dissertation.[13]

The spinline stress was measured near the winder with the help of a hand-held tensiometer. As reported previously in the literature,[11] the stress was found to increase, almost linearly, with the spinning speed. It was, however, not influenced by the spinline temperature profile. Consequently, threadline stresses are not reported in this paper.

Fiber Characterization

The as-spun fiber was characterized with the help of a variety of different experimental techniques.

These included:

Density. A density gradient column filled with a mixture of carbon tetrachloride and toluene at 23°C was used. The samples were left in the column for six hours so that a steady state could be attained. The crystallinity, X, of the fiber was then calculated as:

$$X = \frac{1 - \rho_a/\rho}{1 - \rho_a/\rho_c} \tag{1}$$

where ρ_a and ρ_c are the densities of the purely amorphous and crystalline phases, respectively, and ρ is the measured density of the sample. For PET $\rho_a = 1.335$ g/cc and $\rho_c = 1.455$ g/cc.

Differential Scanning Calorimetry (DSC). A model DSC II Perkin-Elmer differential scanning calorimeter was used to thermally analyze the PET fibers. A typical sample consisted of 5–10 mg of the fiber, and this was scanned from 0°C to 280°C at a rate of 10°C/min. No quantitative estimates of the degree of crystallinity were obtained by this method since the polymer tends to crystallize further during the process of measurement. The technique was mainly used to qualitatively examine the influence of processing conditions on the polymer glass transition temperature, melting point, and the heat of fusion.

Optical Birefringence. A Leitz polarizing microscope was utilized for measuring the total birefringence, Δ_T, of the fiber. This quantity is the difference between the principal refractive index in the stretch direction, $n_{\|}$, and the principal refractive index perpendicular to the stretch direction, $n_{\perp}$.[14] These two refractive indices were measured,[13] in turn, by matching the fiber's refractive index with that of an immersion oil surrounding the fiber.

For a uniaxially oriented polymer, Δ_T can be expressed as sum of contributions from the amorphous and crystalline regions as.[14]

$$\Delta_T = X\Delta_c + (1 - X)\Delta_a \tag{2}$$

where Δ_c and Δ_a are the birefringence contributions from the crystalline and amorphous phases, respectively, and X is the volume fraction of the fiber that is crystalline.

Since X is obtained from density measurements, Eq. (2) provides a relationship between Δ_c and Δ_a. These latter two quantities are usually expressed further as:[14]

$$\Delta_c = f_c\Delta_c^\circ \tag{3}$$

and

$$\Delta_a = f_a\Delta_a^\circ \tag{4}$$

where Δ_c° and Δ_a° are, respectively, the intrinsic birefringences of the crystal-

line and amorphous phases and are material constants (equal to 0.22 and 0.19 in this case). Also f_c and f_a are, respectively, the Hermans orientation functions describing the two phases. While f_c is determined from x-ray diffraction studies, f_a is calculated using Eqs. (2)–(4).

X-ray Diffraction. The fiber samples were scanned by a General Electric XRD-6 diffractometer equipped with a 3° beam slit, medium resolution soller slit, and a 0.2° detector slit. A copper target tube with a nickel filter operating at 45 KVP and 15 mA was used. A specially designed fiber mounting device was made for the X-ray analysis; several layers of fiber, about 1–2 mm thick, were wrapped around a microscope glass slide and mounted on the device. The samples were scanned at various angles between 6° and 50° with the fiber axis oriented at 90° to the axis of rotation of the sample holder. The procedure was repeated with the fiber axis orientation changed to 80°, 70°, 60°, and so on till 0°.

Using the data obtained above, the crystal orientation function is calculated as:

$$f_c = \frac{3\langle \mathrm{Cos}^2\phi_c\rangle - 1}{2} \tag{5}$$

where ϕ_c is the angle between the fiber axis and the molecular chain axis and the average denoted by the pointed brackets is determined as

$$\langle \cos^2\phi\rangle = \frac{\int_o^{\pi/2} I(\phi)\mathrm{Sin}\phi\cos^2\phi d\phi}{\int_0^{\pi/2} I(\phi)\sin\phi\, d\phi} \tag{6}$$

in which $I(\phi)$ is the X-ray intensity. In the present case, the crystallographic plane of $\{\bar{1}05\}$ observed at a Bragg angle of 43° was used to determine the crystalline orientation.

The X-ray diffraction data can also be used to determine the dimension $D\{h\ k\ l\}$ of the crystallites in the fiber samples. According to Scherrer[15]

$$D\{h, k, l\} = \frac{K\lambda}{\beta\,\mathrm{Cos}\,\theta} \tag{7}$$

where $\lambda = 1.5418$ Å, $K = 0.9$, and β is the half maximum line width in radians of the resolved diffraction peak. Peak resolution was carried out by the method described by Hindeleh and Johnson[16] and instrumental broadening of the peak was corrected according to the procedure suggested by Klug and Alexander.[17] While crystal plane $\{\bar{1}05\}$ at $2\theta = 43°$ was used to determine the longitudinal dimension of the crystallites, crystal planes $\{100\}$ at $2\theta = 26°$ and $\{010\}$ at $2\theta = 18°$ were used to calculate the lateral dimensions.

Tensile Testing. Stress-strain curves of the as-spun fibers were generated using a Model 1000 Instron machine. Due to the small diameter of the fibers, an area compensator was used. Also, each datum point was repeated five times.

TABLE I
Spinability of Fiber Under Various Process Conditions

Run #	Mass flow rate (g/min)	Take-up velocity (m/min)	Extrusion temperature (°C)	Spinability
T1	3.50 ± 0.02	240–1500	280	Impossible
T2	2.50 ± 0.03	240–1500	280	Poor
T3	1.20 ± 0.05	240–1500	280	Good
T4	1.00 ± 0.05	240–1500	280	Fair
T5	3.50 ± 0.02	240–1500	285	Impossible
T6	2.50 ± 0.03	240–1500	285	Poor
T7	1.20 ± 0.05	240–1500	285	Good
T8	1.00 ± 0.05	240–1500	285	Fair
T9	3.50 ± 0.02	240–1500	290	Impossible
T10	2.50 ± 0.03	240–1500	290	Poor
T11	1.20 ± 0.05	240–1500	290	Fair
T12	1.00 ± 0.05	240–1500	290	Poor

RESULTS AND DISCUSSION

Both isothermal and nonisothermal spinning of PET were carried out at wind-up speeds of up to 1,500 m/min. Although synthetic textile fibers are manufactured in a nonisothermal manner using cross flow air to cool the filaments which are then wound on a bobbin as multifilament yarn, in the present work only a single filament of circular cross-section was extruded and this was cooled by natural convenction. The purpose of these nonisothermal experiments, done using process conditions similar to those reported in the literature, was to ensure that consistent and expected results could be obtained with the present set-up. A total of twelve nonisothermal runs of a "scouting" nature were conducted initially to judge the spinability of the filament under various process conditions and the results are detailed in Table I. It was found that in order to obtain a stable spinline, a mass flow rate of 1.2 g/min and an extrusion temperature of 285°C had to be used. These same conditions were kept unchanged for the isothermal runs as well for which the filament temperature ranged from 180°C to 240°C. It should be noted that this temperature range encloses the temperature at which the crystallization rate of PET is a maximum under quiescent conditions.[18] The entrance to the isothermal chamber was always located at a distance of 5 cm from the spinneret; this was found to be the optimum from the viewpoint of filament stability (minimizing draw resonance).

Nonisothermal Spinning

The measured spinline diameter profiles for four typical take-up velocities are shown in Figure 2 and the corresponding (calculated) velocity profiles are displayed in Figure 3. The S-shaped curves in the latter figure are characteristic of the velocity profiles found in melt spinning and are consistent with data reported in the literature.[10,19] The temperature profiles for these fibers are presented in Figure 4, and one notices a very sharp drop in temperature initially followed by a much more gradual change later on. The absence of a

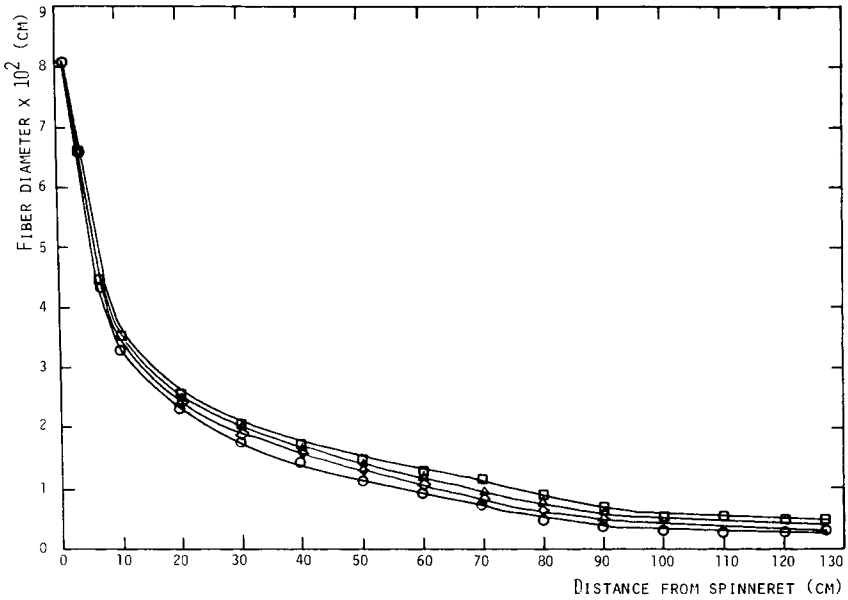

Fig. 2. Diameter profiles of fibers spun under nonisothermal conditions: (○) 1500 m/min; (◇) 1000 m/min; (△) 800 m/min; and (□) 528 m/min.

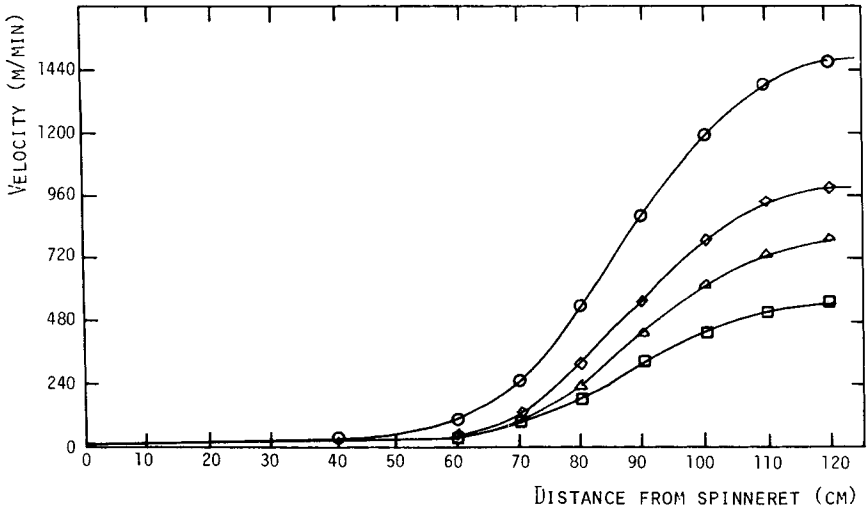

Fig. 3. Velocity profiles of fibers spun under nonisothermal conditions: (○) 1500 m/min; (◇) 1000 m/min; (△) 800 m/min; and (□) 528 m/min.

plateau in the temperature profile indicates that little or no crystallization is taking place. Also, as reported by others,[20] the spinline corresponding to the maximum wind-up speed cools most rapidly.

On analyzing the as-spun fibers, it was found that the maximum crystallinity, even at the highest spinning speed, was about 10% and this was influenced little by the mass flow rate or the extrusion temperature. In essence, amorphous fibers were obtained, and this was entirely as expected. This conclusion was reinforced by the DSC results which are shown in Figure 5. Both a cold crystallization peak and a fusion peak were observed at each spinning speed

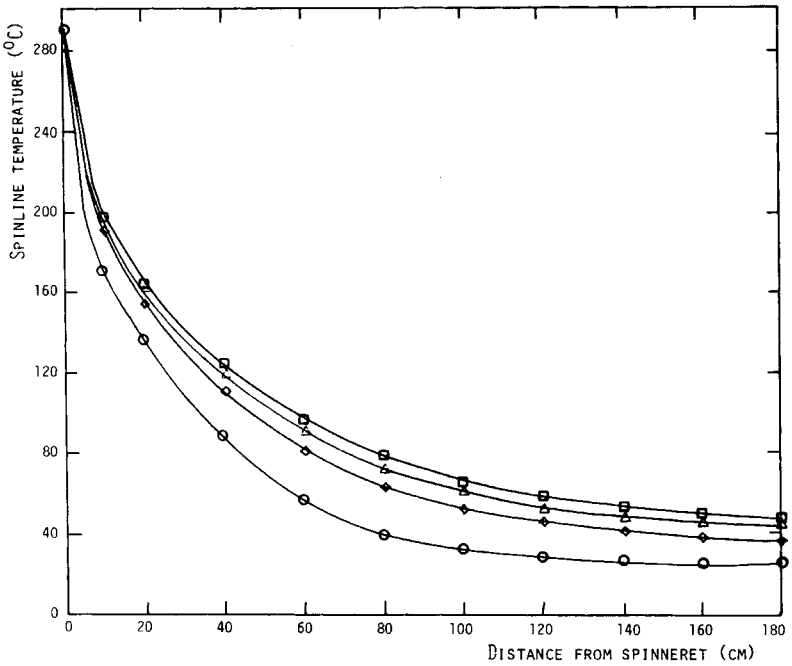

Fig. 4. Temperature profiles of fibers spun under nonisothermal conditions: (○) 1500 m/min; (◇) 1000 m/min; (△) 800 m/min; and (□) 528 m/min.

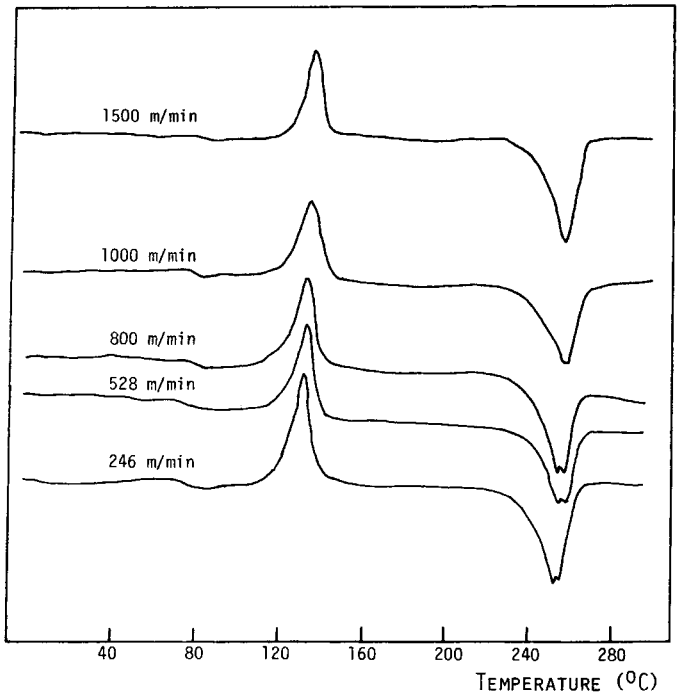

Fig. 5. Differential scanning calorimeter results for the nonisothermal fibers.

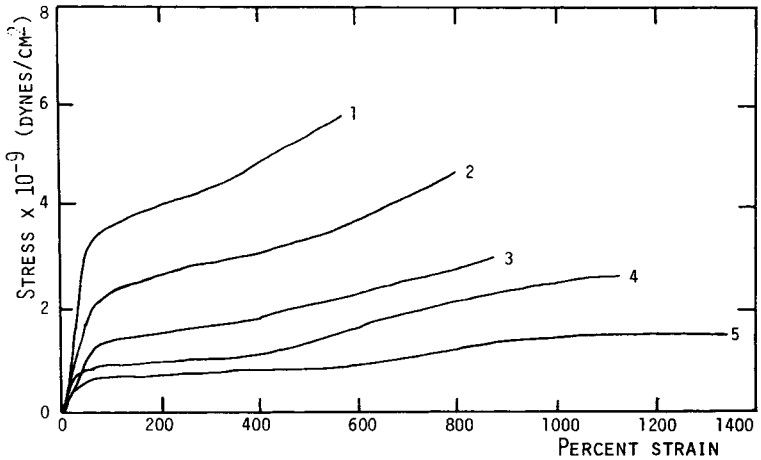

Fig. 6. Stress-strain curves of the nonisothermal fibers. The take-up speeds are: (1) 1500 m/min; (2) 1000 m/min; (3) 800 m/min; (4) 528 m/min and (5) 246 m/min.

and the areas under these were equal suggesting that all the crystallization took place during the process of measurement. Furthermore, the glass transition temperature was unchanged at about 75°C as the spinning speed was varied. The X-ray diffraction patterns gave no additional information, and only dome shaped curves were observed at all speeds. Simultaneously, the measured birefringence was found to be small in all cases and the calculated orientation functions had values less than 0.1. The stress-strain curves are shown in Figure 6 and even though the mechanical strength increased with spinning speed, the ultimate strength remained low.

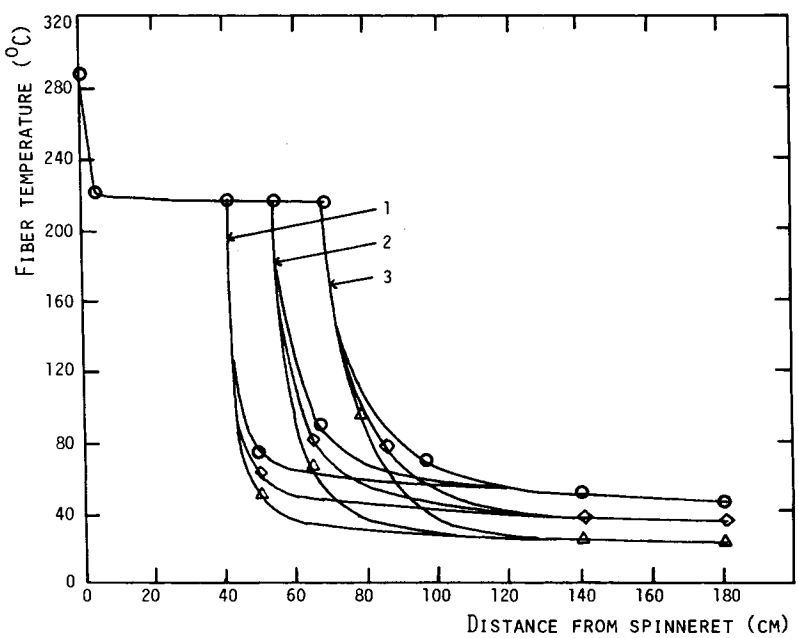

Fig. 7. Measured spinline temperature profiles for different isothermal oven lengths: (1) 41 cm; (2) 53 cm; (3) 68 cm; (○) 1500 m/min; (◇) 1000 m/min; and (△) 800 m/min.

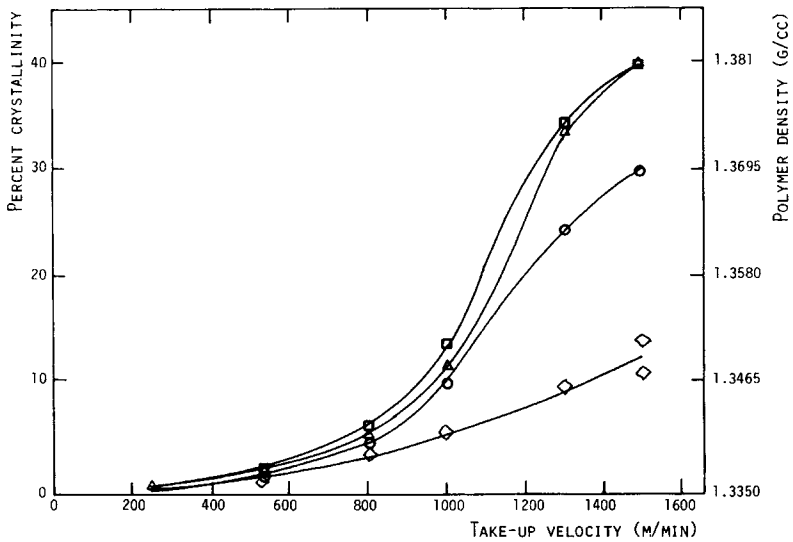

Fig. 8. Effect of temperature and take-up speed on the fiber crystallinity: (○) 200° C; (□) 220° C; (△) 240° C; and (◇) nonisothermal.

Isothermal Spinning

The filament diameter and velocity profiles in isothermal melt spinning were found to be qualitatively similar to those in Figures 2 and 3, and are, therefore, not shown. One major difficulty encountered in isothermal spinning was the instability of the spinline. Depending on the spinline temperature,

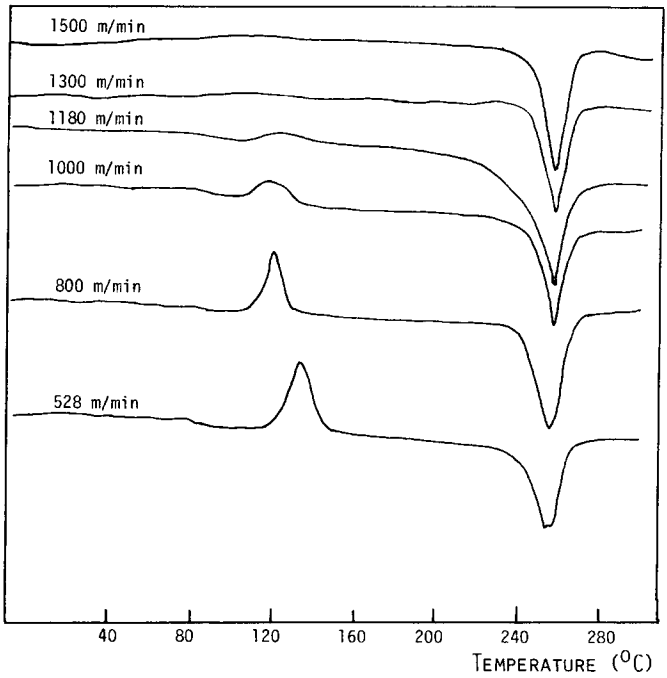

Fig. 9. Differential scanning calorimeter results for fibers spun at 220°C.

location, and length of the isothermal oven, an unstable filament undergoing draw resonance could be generated. Numerous trial runs had to be conducted to determine the optimum settings for a stable operation. Typical temperature profiles corresponding to different oven lengths and wind-up speeds are shown in Figure 7 for a fiber temperature of 220°C. Results at other temperatures were similar.

The variation of crystallinity with spinning speed at three different temperatures is shown in Figure 8 for the longest oven length. It is seen that very considerable amounts of crystallinity are obtained, especially as the wind-up speed is increased. Also, at a given speed, the percentage crystallinity goes through a maximum with increasing temperature. This is similar to the behavior exhibited by quiescent crystallization; the temperature at which the highest crystallization rate occurs, though, is higher in the presence of stress. Such behavior has been reported previously.[9] In comparing these results to those obtained under nonisothermal conditions, and also displayed in Figure 8, it is found that the crystallinity level is about four times greater at the

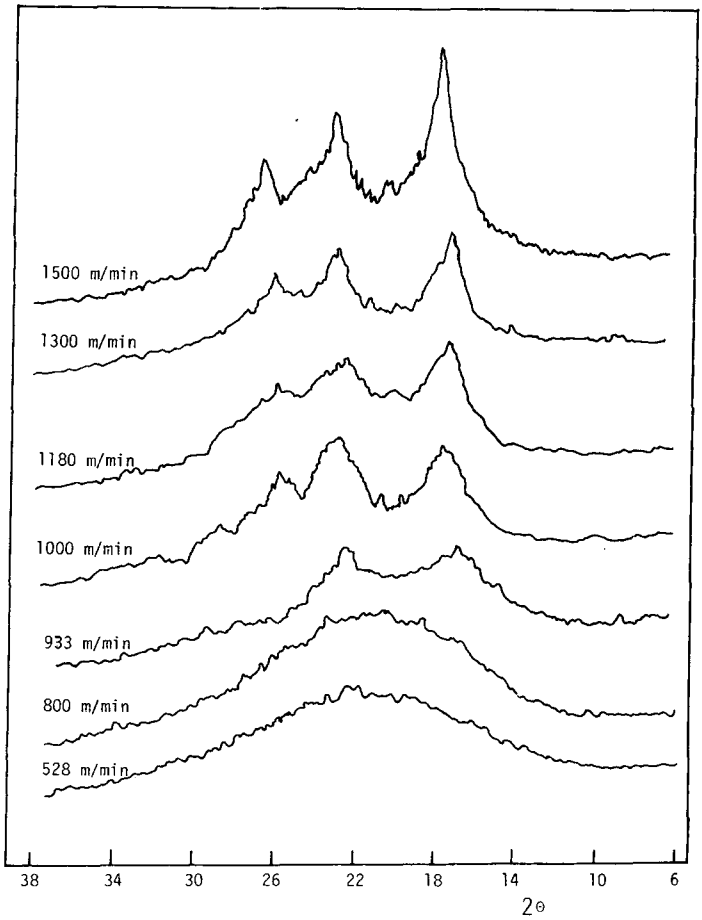

Fig. 10. X-ray diffraction curves for fibers spun at 220°C.

highest spinning speed. The maximum crystallinity obtained is about 40% and this figure is more characteristic of commercial high speed spinning[21] than the low speed spinning used here. Also, as far as the rate of crystallization is concerned, the rates obtained here are much greater than those for both optimum isothermal quiescent crystallization[18] and nonisothermal crystallization on the spinline.

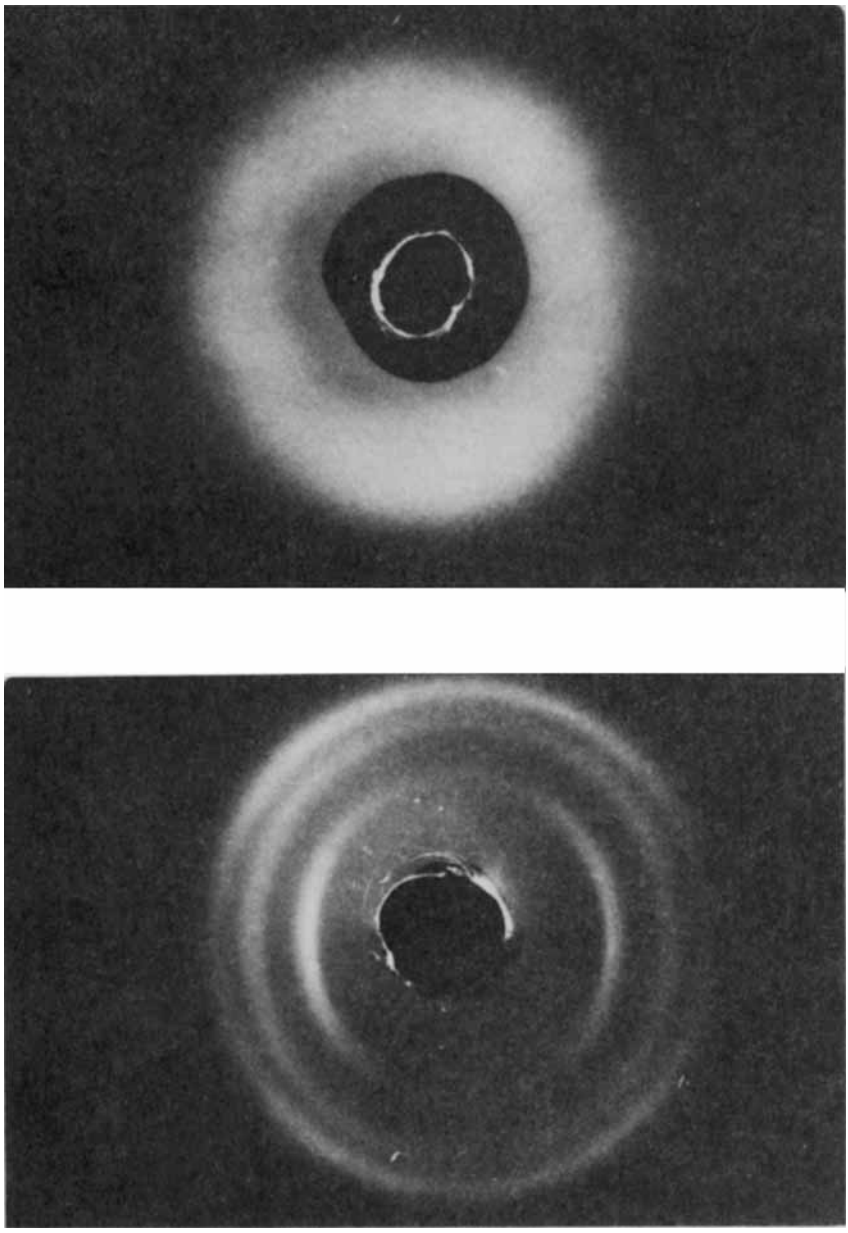

Fig. 11. WAXS results for (a) nonisothermally spun fiber at 1500 m/min and (b) isothermally spun fiber at 1500 m/min and 220°C.

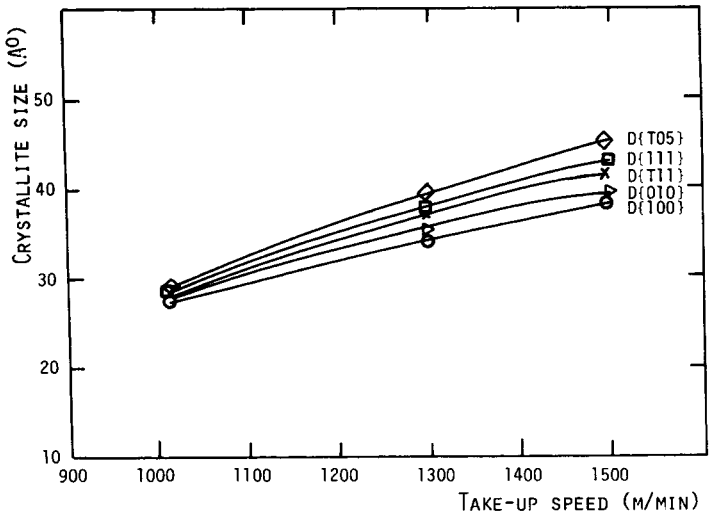

Fig. 12. Crystallite sizes as a function of spinning speed for fibers made at 220°C.

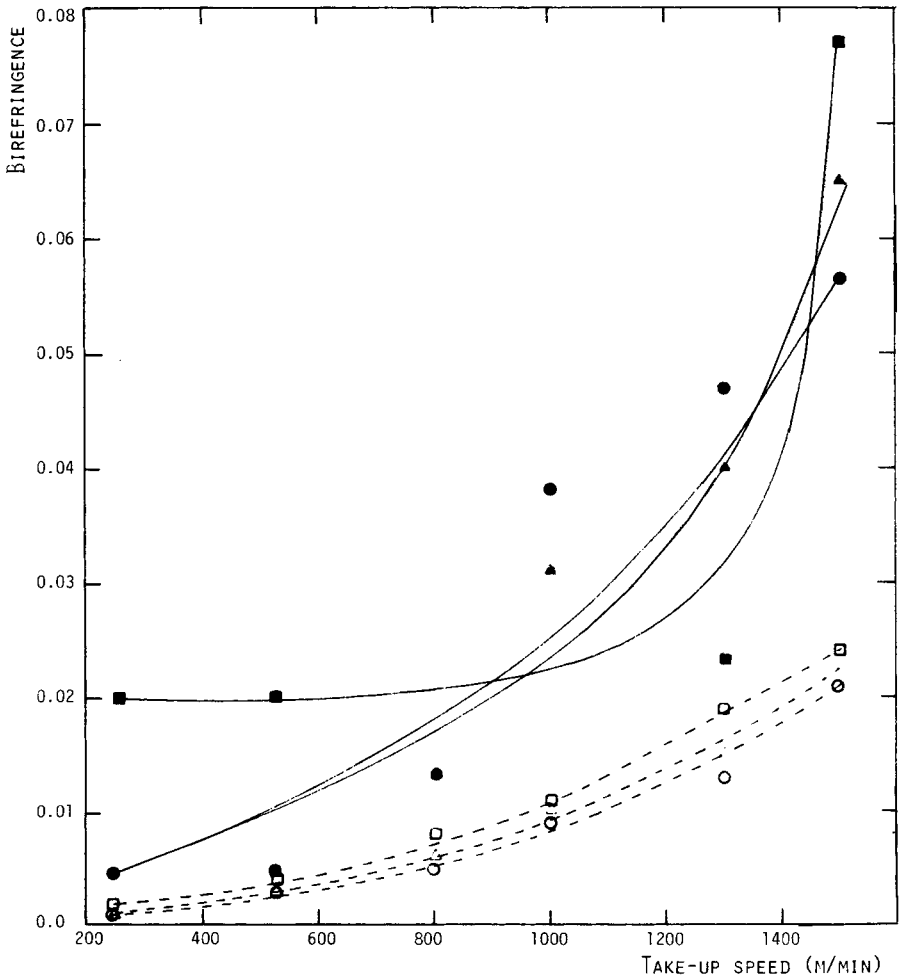

Fig. 13. Influence of spinning speed and temperature on the birefringence: (△) overall birefringence; (□) crystalline birefringence; and (○) amorphous birefringence. Solid lines are data at 220° C while broken lines are nonisothemal results.

Further evidence of the high crystallinity levels is found in the DSC curves presented in Figure 9. Shown are the results for fibers spun at 220°C using the longest oven length (maximum residence time) as a function of the spinning speed. That the crystallinity increased with wind-up speed is clear from the progressive decrease in the height of the cold crystallization peak and its eventual disappearance and also by the upward movement of the glass transition temperature.

The X-ray diffraction patterns of isothermally spun fibers showed distinct crystalline peaks (Figure 10) which were not found in the nonisothermal case. As the isothermal spinline temperature changed from 180°C to 240°C, the crystal peaks became larger and sharper. This is an indication of the gradual development of crystallinity in the fiber brought about by changes in the process conditions. To confirm these findings, wide angle X-ray scatterings were done at the University of Tennessee for samples spun under nonisothermal and isothermal conditions. The results are displayed in Figure 11. While a diffuse halo was obtained for the nonisothermal fiber, clear sharp arcs were observed with the isothermal fiber. These arcs are commonly encountered in crystalline and oriented fibers.

X-ray diffraction data were used to determine the crystallite size according to Eq. (7), and the results are shown in Figure 12 at a single temperature. The longitudinal dimensions were only slightly greater than the lateral ones and were of the same order of magnitude as those for nonisothermal, high speed spinning as reported by Heuvel and Huisman.[10] Also, while the crystallite size increased with spinning speed in the range of spinning speeds considered here, it showed a maximum with regards to the temperature.

The birefringence and orientation of these isothermally spun fibers were measured with the polarizing microscope and the X-ray diffractometer. The results are shown in Figures 13 and 14. On comparing these to literature data,[10,11,19,21] it is found that these orientation levels would generally be found in fibers spun at much greater speeds (3,500-4,500 m/min) than those

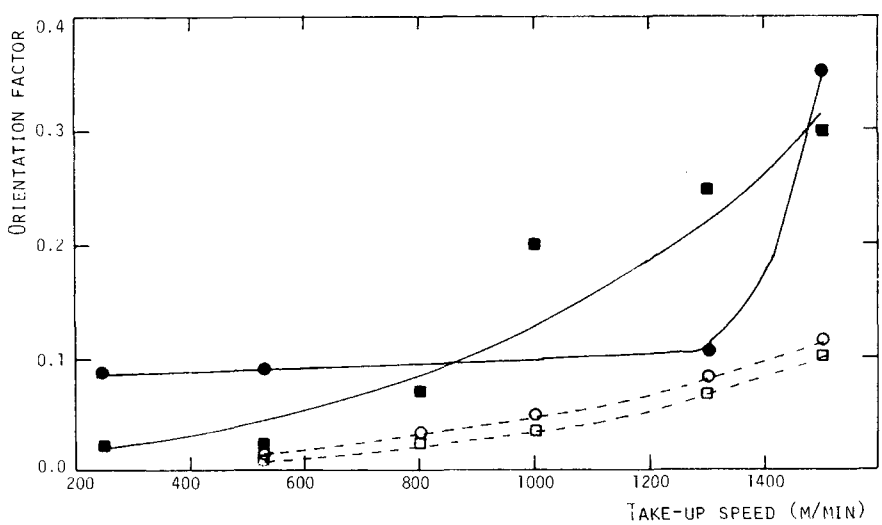

Fig. 14. Crystalline (○) and amorphous (□) orientation factors corresponding to data shown in Figure 13.

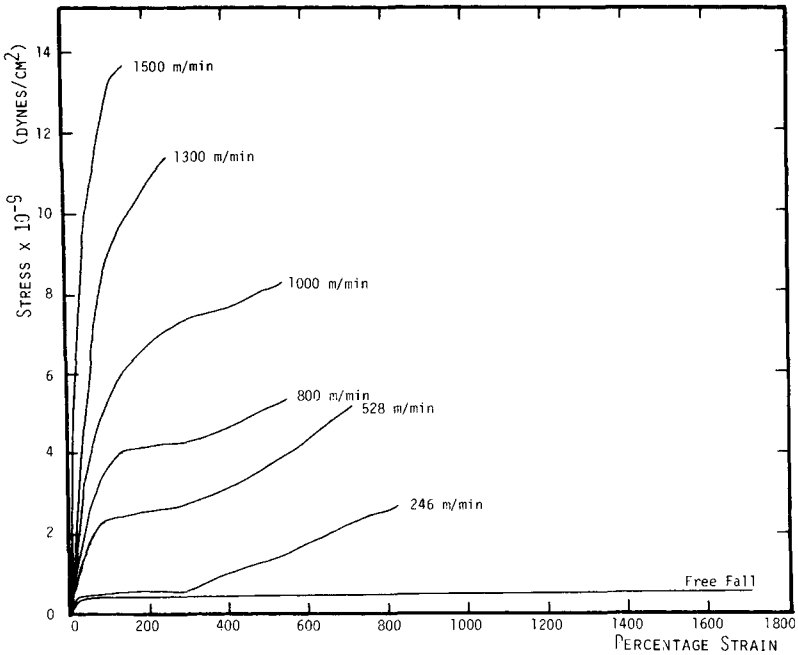

Fig. 15. Stress-strain curves of fibers made at 220°C.

employed here. In fact, to the best of our knowledge, there is no published work on PET melt spinning at such low speeds where similar results have been obtained.

The stress-strain curves of the isothermally spun fibers are presented in Figure 15 and these can be compared and contrasted with those shown earlier in Figure 6. The shapes of the former curves vary with wind-up speed with the low speed curves exhibiting ductile behavior and long elongations before break. Concomitantly, the ultimate strength is very low and this is typical of an amorphous fiber. At higher spinning speeds, the fiber gains molecular orientation and crystallinity and its mechanical properties improve. The fiber becomes much less ductile, the modulus increases and so does the ultimate strength. Qualitatively similar behavior is obtained at other temperatures as well.

CONCLUDING REMARKS

The work presented here shows that it is possible to drastically alter the physical structure of a polymeric solid by changing the process conditions. In polymer melt spinning, in particular, a control of the spinline temperature makes it possible to spin amorphous, unoriented fibers or oriented crystalline ones. This work contributes to our understanding of structure development in polymers, a knowledge which can ultimately be used for economic gain.

This research was financed, in part, by the National Science Foundation through grant number CPE-8204092. The WAXS patterns shown in Figure 11 were obtained courtesy of Professor J. E. Spruiell. The authors have also benefitted from discussions with Professor A. B. Metzner of the

University of Delaware, Mr. R. L. Ballman and Dr. J. H. Southern of the Monsanto Company, and Drs. S. Abdalla, M. Deeg, and K. F. Wissbrun of the Celanese Research Company. The polymer used in this work and parts of the fiber spinning setup were gifts by Celanese. This is gratefully acknowledged.

References

1. L. Mandelkern, *Crystallization of Polymers*, McGraw Hill, New York, 1964.
2. D. W. van Krevelen, *Chimia*, **32**, 279–294 (1978).
3. D. C. Bassett, *Principles of Polymer Morphology*, Cambridge University Press, Cambridge, 1981.
4. J. H. Southern (Ed.), special issue on "Stress Induced Crystallization," *Polym. Eng. Sci.*, **16**(3), 125–228 (1976).
5. W. T. Mead (Ed.), Symposium issue on Crystallinity Control and Polymer Mechanics, *Polym. Eng. Sci.*, **18**, 429–548 (1978).
6. W. B. Black and W. L. Wu (Eds.), Symposium issue on Stress Induced Crystallization, part II, *Polym. Eng. Sci.*, **19**, 385–468 (1979).
7. R. L. Miller (Ed.), *Flow Induced Crystallization in Polymer Systems*, Gordon and Breach Science Publishers, New York, 1979.
8. J. R. Dees and J. E. Spruiell, *J. Appl. Polym. Sci.*, **18**, 1053 (1974).
9. V. M. Nadkarni and J. M. Schultz, *J. Polym. Sci., Polym. Phys. Ed.*, **15**, 2151 (1977).
10. H. M. Heuvel and R. Huisman, *J. Appl. Polym. Sci.*, **22**, 2229 (1978).
11. S. K. Garg, *J. Appl. Polym. Sci.*, **29**, 2111 (1984).
12. A. Ziabicki, in *High Speed Fiber Spinning*, A. Ziabicki and H. Kawai, Eds., Wiley, New York, 1985.
13. K. F. Auyeung, Ph.D. dissertation, Chemical Engineering, State University of New York at Buffalo, 1986.
14. R. J. Samuels, *Structured Polymer Properties*, John Wiley, New York, 1974.
15. P. Scherrer, *Gottingher Nachrichten*, **2**, 98 (1918).
16. A. M. Hindeleh and D. J. Johnson, *Polymer*, **19**, 27 (1978).
17. H. P. Klug and L. E. Alexander, *X-ray Diffraction Procedures for Polycrystalline and Amorphous Materials*, John Wiley, New York, 1954.
18. W. H. Cobbs and R. L. Burton, *J. Polym. Sci.*, **10**, 275 (1953).
19. G. Bragato and G. Gianotti, *Eur. Polym. J.*, **19**, 795 (1983).
20. J. E. Spruiell and J. L. White, *Appl. Polym. Symp.*, **27**, 121 (1975).
21. A. Ziabicki, Proc. Fiber Producer Conf., Greenville, SC, p. 2-1, 1984.

Received September 5, 1986
Accepted January 10, 1987